IOPscience iopscience.iop.org

Home Search Collections Journals About Contact us My IOPscience

X-ray photoemission studies of praseodymium thin films on SiO_2/Si(100)

This article has been downloaded from IOPscience. Please scroll down to see the full text article.

2003 J. Phys.: Condens. Matter 15 5857

(http://iopscience.iop.org/0953-8984/15/34/315)

View the table of contents for this issue, or go to the journal homepage for more

Download details:
IP Address: 171.66.16.125
The article was downloaded on 19/05/2010 at 15:06

Please note that terms and conditions apply.

INSTITUTE OF PHYSICS PUBLISHING JOURNAL OF PHYSICS: CONDENSED MATTER

J. Phys.: Condens. Matter **15** (2003) 5857–5864 PII: S0953-8984(03)62507-5

X-ray photoemission studies of praseodymium thin films on SiO_2/Si(100)

J X Wu, Z M Wang, M S Ma and S Li

Structure Research Laboratory, University of Science and Technology of China, Hefei 230026, People's Republic of China

E-mail: wujx@ustc.edu.cn

Received 22 April 2003
Published 15 August 2003
Online at stacks.iop.org/JPhysCM/15/5857

Abstract

Pr overlayers, with thicknesses of about 1.8 and 0.6 nm, were deposited on 1.2 nm SiO_2/Si(100) at room temperature and x-ray photoelectron spectroscopy (XPS) was used to investigate the reactions at the Pr/SiO_2/Si interfaces as a function of annealing temperature. The results show that the Pr overlayers reduce SiO_2 at room temperature, forming Pr_2O_3 and a Pr silicate (Pr–O–Si). For the 1.8 nm Pr/SiO_2/Si system, the 1.2 nm SiO_2 layer is mostly reduced at room temperature and a Pr silicide was also observed. The Pr–O–Si silicate increases in intensity while the Pr_2O_3 intensity decreases with annealing temperature. Angle-dependent XPS, taken after annealing, indicates that the silicate is located at the top surface. In the case of the 0.6 nm Pr/SiO_2/Si system, the Pr overlayer is almost oxidized after annealing, and some SiO_2 remains even after annealing at 1090 K, which can serve as a low-defect-density buffer layer between the high-κ film (Pr_2O_3 and Pr–O–Si) and the silicon.

1. Introduction

As the dimensions of complementary metal oxide semiconductor (CMOS) devices are reduced, the thickness of the silicon dioxide layer as a gate dielectric will soon reach the physical limit [1, 2]. High dielectric constant materials are needed to replace the traditional SiO_2 in future CMOS devices, so a search for alternative gate dielectrics has focused on metal oxides and their silicates [3, 4]. Because the candidates for the gate dielectrics must have excellent interfacial properties with silicon, the interfaces between high-κ materials and Si have been studied intensively. Hafnium, zirconium and praseodymium oxides and their silicates have attracted much attention due to their reasonably large dielectric constants, high conduction band offsets and thermodynamic stability on silicon [4–8]. Because the interfacial state densities between high-κ materials and silicon are higher than that observed in the SiO_2/Si system, it is preferrable to have a few monolayers of SiO_2 serving as a low-defect-density bottom oxide between the high-κ film and the silicon [9].

© 2003 IOP Publishing Ltd Printed in the UK

In this work, the Pr overlayers with thicknesses of about 1.8 and 0.6 nm were deposited on 1.2 nm SiO_2/Si(100) at room temperature, and *in situ* XPS was used to investigate the Pr/SiO_2/Si interfaces as a function of annealing temperature. It is known that SiO_2 can be reduced by some metals [10, 11], forming metal oxides. The crystalline praseodymium oxide films of Pr_2O_3-type grown on Si(100) have outstanding electrical properties, with a dielectric constant of 31 and an ultra-low leakage current density [12]. As XPS is a powerful technique for determining the chemical states of elements at or near the surface, the interfacial reactions in the Pr/SiO_2/Si system were monitored by Si 2p, O 1s and Pr 3d core-level spectra. The results show that SiO_2 can be reduced by the Pr overlayer, forming Pr_2O_3 and a Pr–O–Si silicate. The silicate grows and the Pr_2O_3 intensity decreases with annealing temperature.

2. Experiment

The experiments were carried out in an ESCALAB MK II system, with a base pressure of 2×10^{-8} Pa. An Al Kα radiation source ($h\nu = 1486.6$ eV) was used in XPS measurements. The analyser was in the constant resolution mode at a pass energy of 20 eV. Photoelectrons were collected at an emission angle of 15° with respect to the surface normal. The samples were n-type Si(100), covered by a native SiO_2 overlayer and some carbon contamination. The samples were annealed at 1100 K for several cycles by using resistive heating to remove carbon contamination, leaving the native SiO_2 layer on the Si(100). The physical vapour Pr deposition was undertaken by passing a current through a tungsten basket containing a piece of Pr (99.7%). The annealing temperature was estimated from the heating current according to a current–temperature calibration curve, and the annealing time at each temperature was 15 min.

3. Results and discussion

Figure 1(a) shows the evolution of Si 2p core-level spectra upon Pr deposition and post-annealing for the SiO_2/Si(100) surface covered by a 1.8 nm Pr overlayer. A mixed Gaussian/Lorentzian function was used to decompose the Si 2p spectra [13]. It is known that there are four components in the Si 2p core-level spectrum due to chemical shift, corresponding to silicon atoms bonded to one, two, three and four oxygen atoms (Si^{1+}, Si^{2+}, Si^{3+} and Si^{4+}), respectively [14, 15]. Before Pr deposition, the Si 2p core-level spectrum, at the bottom of figure 1(a), was fitted using four peaks: Si^0 (substrate) at 99.6 eV, Si^{1+} at 100.4 eV, Si^{2+} at 101.3 eV, and Si^{4+} at 103.9 eV, with a full width at half maximum (FWHM) of 1.4 ± 0.1 eV for peaks 1–3 and 2.0 ± 0.1 eV for peak 4, respectively. The feature at 103.9 eV is typical of SiO_2 (Si^{4+}). We attribute Si^{1+} and Si^{2+} to the silicon atoms arising from the SiO_2/Si interface. The area ratio between the Si 2p core levels of Si^0 and Si^{4+} was 4.7, which can be used to estimate the thickness of the SiO_2 overlayer [16]. The oxide thickness was estimated to be about 1.2 nm by assuming that the mean free paths of the Si 2p photoelectrons are 3.2 and 3.7 nm in the substrate and the oxide, respectively [16]. The energy separation (4.3 eV) between the Si 2p core levels of Si^0 and Si^{4+} as well as the oxide thickness (1.2 nm) in this work are in very good agreement with the values given in the literature [9]. The corresponding O 1s core level for SiO_2, shown in figure 2(a), has a binding energy of 533.2 eV.

After Pr deposition, the Si 2p intensity of the substrate was reduced to 0.51 of its value for the SiO_2/Si surface. Because there is a strong reaction between the Pr overlayer and SiO_2 at room temperature (see below), the island mode for overlayer growth can be excluded in this system [10]. The thickness of the Pr overlayer was estimated by using the attenuation

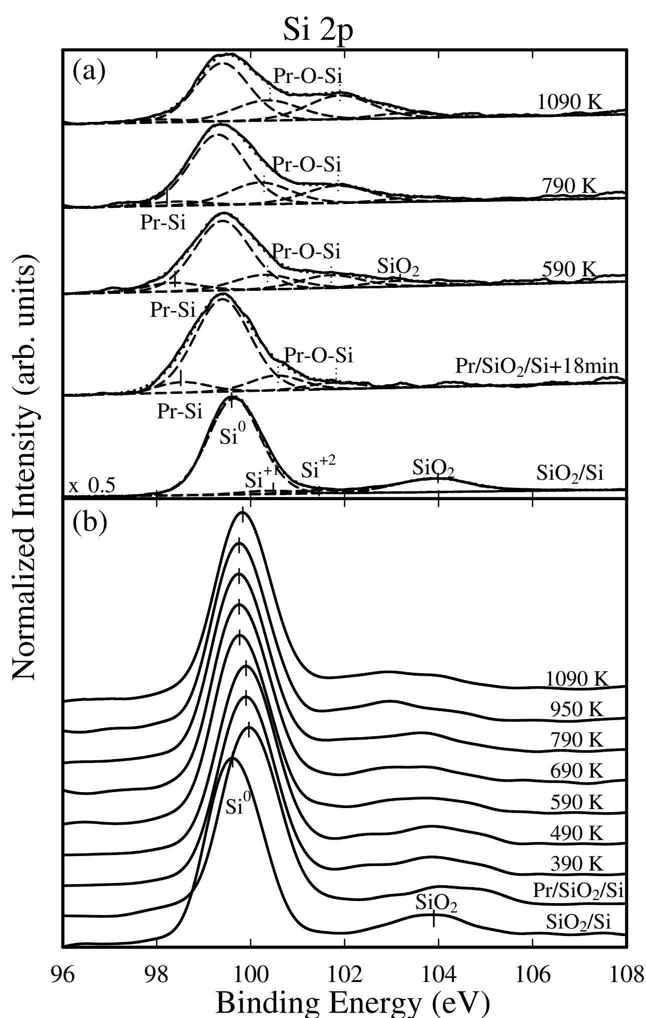

Figure 1. The evolution of the Si 2p core-level spectra upon Pr deposition and post-annealing for (a) the 1.8 nm Pr/SiO_2/Si surface and (b) the 0.6 nm Pr/SiO_2/Si surface.

of the Si 2p core level and the mean free path of 2.8 nm for the Si 2p photoelectrons in the Pr overlayer [13]. The evolution of the O 1s core-level spectra over time is also given in figure 2(a). For the as-evaporated Pr surface, the O 1s spectrum shows that the emission of SiO_2 decreases in intensity and that new features around 530.8 and 532.3 eV appear. It was found that the Pr deposition results in 0.4–0.7 eV shifts of the Si 2p and O 1s core levels to higher binding energies. After keeping the sample at room temperature for 18 min, we can see that the O 1s emission of SiO_2 almost disappears. Meanwhile, the O 1s peaks move to lower binding energy. The O 1s core-level spectrum can be fitted by two components at 530.4 and 531.6 eV, which can be attributed to Pr_2O_3 and a Pr–O–Si silicate [8], respectively. The Pr–O–Si silicate has previously been observed at the Pr_2O_3/Si interface [6, 8]. As the Pr 4d core level has a broad peak around 115 eV, its satellites resulted from Al K$\alpha_{3,4}$ overlap with the Si 2p signal. The Si 2p spectra taken after Pr deposition in figure 1(a) were processed by removing the satellites. The Si 2p spectrum obtained after Pr deposition for 18 min exhibits

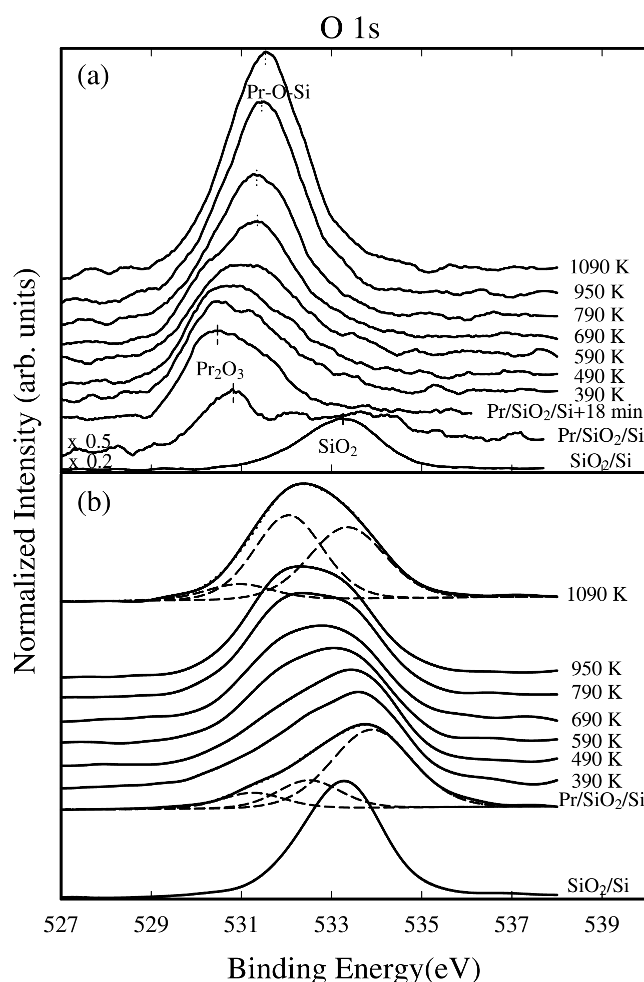

Figure 2. The O 1s core-level spectra corresponding to the same conditions as in figure 1.

at least four features, with binding energies of 98.6, 99.4, 100.5 and 101.8 eV, respectively. The first line, located at 0.8 eV lower than the substrate Si 2p level, is attributed to a Pr–Si silicide [17]. The species at 100.5 and 101.8 eV can be assigned to the silicon atoms bonded to one and two oxygen atoms, respectively, in the form of the Pr–O–Si silicate. One should note that the Si 2p peak due to SiO_2 almost disappears. Since the Si 2p intensity ratio of the substrate to the others is comparable to that of the SiO_2/Si surface, we argue that the 1.2 nm SiO_2 layer is reduced by the Pr overlayer, forming the silicide, silicate and Pr_2O_3. The corresponding spectrum at the bottom of figure 3(a) shows that the Pr $3d_{5/2}$ core level has a binding energy of 932.7 eV, with an FWHM of 4.5 eV, and that the O KLL Auger line is located at 972.7 eV. We argue that metallic Pr is dominant, as the line shape of the Pr 3d core levels is similar to that of Pr overlayer on Si. The O KLL Auger line mainly arises from Pr_2O_3.

As can be seen in figure 1(a), the Si 2p peak of the silicide decreases while the emission of the silicate grows with annealing temperature. The feature at 103.3 eV, which is characteristic of SiO_2, becomes detectable after annealing. Figure 2(a) shows that the total O 1s intensity increases and that the peak due to the silicate grows with temperature. The silicate becomes

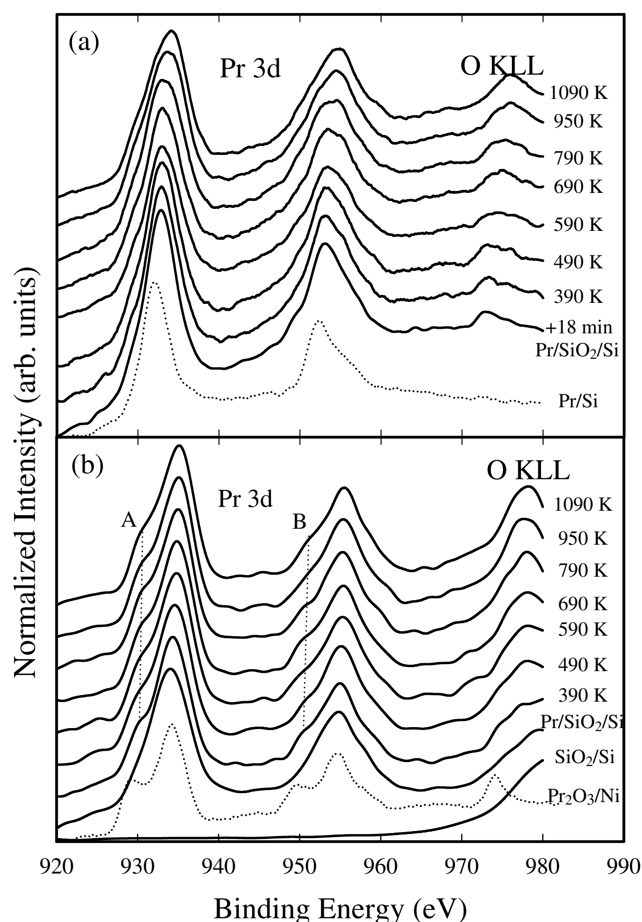

Figure 3. Pr 3d core-level and O KLL Auger spectra taken before and after annealing for (a) the 1.8 nm Pr/SiO_2/Si surface and (b) the 0.6 nm Pr/SiO_2/Si surface. The Pr 3d curves (dotted curves), taken from the Pr/Si and Pr_2O_3/Ni surfaces, are also given in (a) and (b), respectively, for comparison.

dominant after annealing at 690 K. Figure 3(a) shows that annealing results in broadening of the Pr 3d and O KLL peaks. The Pr 3d $3d_{5/2}$ core level has a binding energy of 933 eV in the temperature range 390–590 K and finally shifts to 934.2 eV. The O KLL line gradually moves to 976.0 eV, which can be attributed to the silicate.

In figure 4 we present the Si 2p XPS spectra at emission angles of 0°, 30°, 45° and 60° with respect to the surface normal, respectively, taken after annealing at 950 K. The Si 2p peaks at 99.4 eV were normalized to the same height to show the variations in the line shape. It is evident that the component due to the silicate grows with emission angle. As the spectrum at 60° is more sensitive to the surface, we can conclude that the silicate is located at the top surface. The inset of figure 4 shows the integrated photoemission intensities of the Pr 3d, O 1s and Si 2p (Si^0 and Pr–O–Si) peaks as a function of emission angle. Both the Pr 3d core level and the Si 2p line at 99.4 eV decrease in intensity, while the signals of the silicate and oxygen grow with angle. This behaviour further supports the contention that the silicate is located at the top surface. As the line shape of the Pr 3d spectra in figure 3(a) are dominated by metallic Pr, the metallic Pr atoms may be present under the silicate layer.

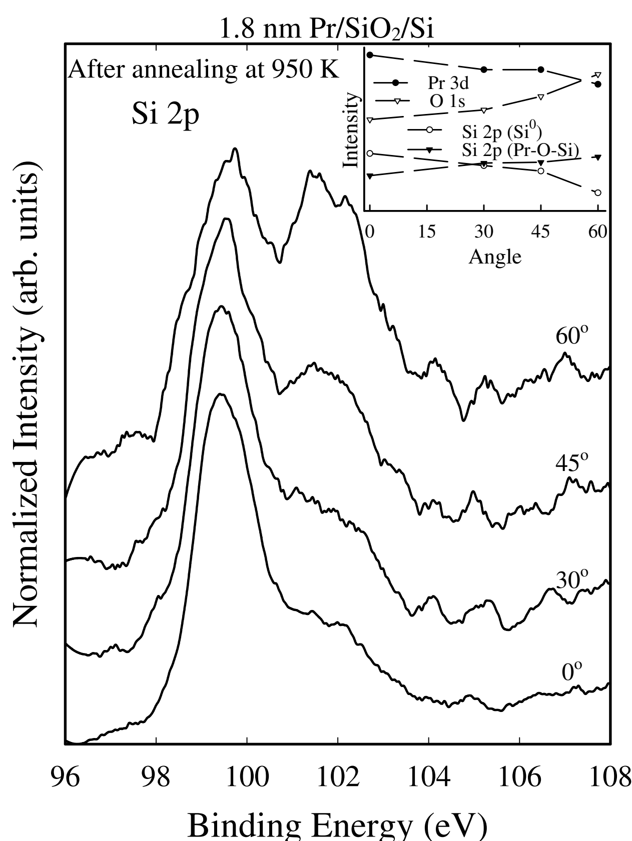

Figure 4. Si 2p core-level spectra at emission angles of 0°, 30°, 45° and 60° with respect to the surface normal, respectively, taken after annealing at 950 K. The Si 2p peaks at 99.4 eV were normalized to the same height. The inset shows the integrated photoemission intensities of the Pr 3d, O 1s and Si 2p (Si^0 and Pr–O–Si) peaks as a function of collecting angle.

Figure 5(a) displays the integrated photoemission intensities of the Pr 3d, Si 2p and O 1s core levels for the 1.8 nm Pr/SiO_2/Si surface as a function of annealing temperature. The Pr 3d intensity decreases while the O 1s signal increases with annealing temperature, which can be attributed to the gradual movement of the Pr oxide and silicate from the interface between the Pr overlayer and Si substrate to the top surface. From the curve of Si 2p, we can see that initial slight growths are followed by slow reductions. The initial slight growths of the Si 2p signal may be related to the accumulation of the Pr silicate on the top surface. Figure 5(b) shows the Si 2p intensities of three different Si species versus annealing temperature. The emission from the substrate is attenuated and the silicate increases in intensity with annealing temperature. The amount of SiO_2 stays almost constant during annealing. It seems that annealing facilitates the bonding of more silicon atoms to oxygen, forming a thicker overlayer and leading to the strong attenuation of emission from the substrate. The slow reduction in the Si 2p intensity at higher temperatures in figure 5(a) may be associated with the attenuation. Figure 5(c) shows the intensity variations of the three oxygen species with temperature. The silicate increases in intensity with temperature, while the intensity of Pr_2O_3 starts to come down at temperatures over 590 K.

Figures 1(b), 2(b) and 3(b) display the spectral evolution of the Si 2p, O 1s and Pr 3d core levels with annealing temperature for the 1.2 nm SiO_2/Si surface covered by a 0.6 nm

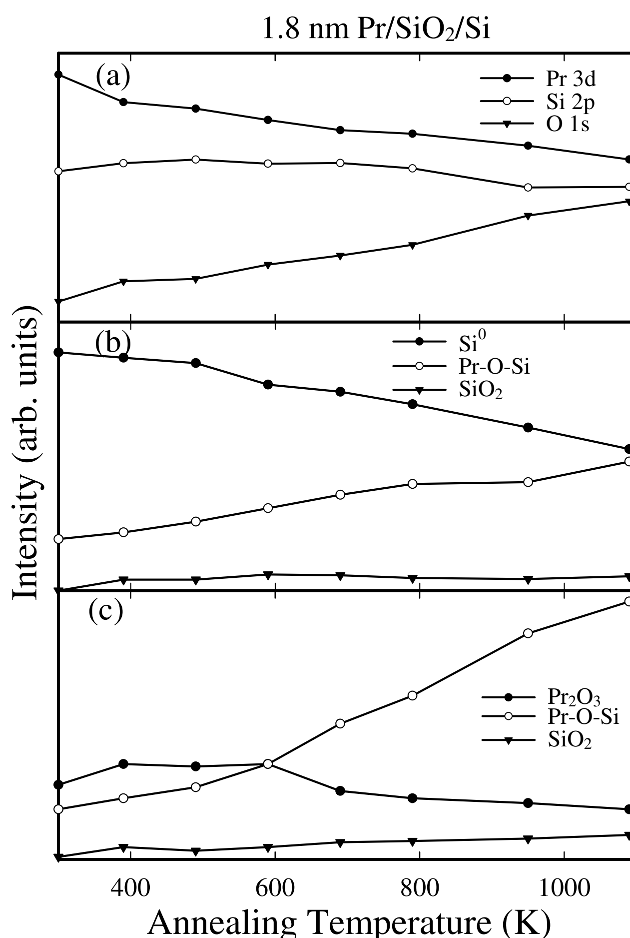

Figure 5. (a) The integrated photoemission intensities of the Pr 3d, Si 2p and O 1s core levels as a function of annealing temperature. (b) The intensity variations of the three different Si components. (c) The intensity variations of the three O 1s peaks.

Pr overlayer. The Pr deposition results in a 0.4 eV shift of the bulk Si 2p peak to higher binding energy and a broadening of the Si 2p feature at higher binding energy. The O 1s spectrum, taken after Pr deposition, has been fitted by three components at 531.3, 532.5 and 533.8 eV, respectively, attributed to the emission from Pr_2O_3, Pr–O–Si and SiO_2. It is evident that some SiO_2 is reduced by the Pr overlayer, forming the Pr silicate as well as Pr_2O_3. The corresponding Pr 3d spectrum in figure 3(b) is mainly due to metallic Pr. Two structures at 930.6 eV (labelled A) and 950.8 eV (labelled B), characteristic of the Pr oxide [8], become visually apparent after annealing. The O KLL line is located at about 979.3 eV for SiO_2 and moves to 977.8 eV after annealing at temperatures over 790 K. The Si 2p and O 1s core levels in figures 1(b) and 2(b) gradually move back to lower binding energy with annealing temperature. As annealing temperature increases, the curve-fitting results of the O 1s spectra indicate that the O 1s peak due to the silicate grows and that the intensities of SiO_2 and Pr_2O_3 decrease. Some SiO_2 remains on the surface even after annealing at 1090 K. The comparison of the Si 2p spectra before Pr deposition and after annealing at 1090 K further indicates that SiO_2 is partly reduced. Angle-dependent XPS taken after annealing at 1090 K (not shown

here) demonstrates that the silicate is located at the top surface. The SiO_2 layer that remains after annealing can serve as a low-defect-density buffer between the high-κ film (Pr_2O_3 and Pr–O–Si) and Si.

From figures 1(b) and 2(b), we note that the bulk Si and SiO_2 features move to higher binding energies by 0.4 and 0.6 eV, respectively, after Pr deposition. The O 1s core levels of Pr_2O_3 and Pr–O–Si, however, are 0.9 eV higher than those observed in the 1.8 nm Pr/SiO_2/Si system. Considering that the work function of a metallic Pr overlayer is much lower than that of silicon, we argue that the shifts are associated with the electron transfer from the Pr overlayer into the SiO_2–Si interface, caused by the difference in work function between the metal overlayer and Si in the metal–insulator–semiconductor structure. This behaviour leads to band bending and the formation of an electric field across the SiO_2 layer. The shift of the bulk Si 2p peak results from the band bending, while the shift of the SiO_2 core levels is attributed to both the band bending and the electric-field gradient across the SiO_2 layer. The broadening of the SiO_2 core levels caused by the electric-field gradient can be seen in figures 1(b) and 2(b). The O 1s core-level shifts of the Pr oxide and silicate are mainly associated with the electric field across the SiO_2 layer. The shifts caused by Pr deposition decrease after annealing and almost disappear after the metallic Pr is oxidized completely (figures 1(b) and 2(b)) or after SiO_2 is reduced completely (figure 2(a)).

4. Conclusions

Pr overlayers with thicknesses of about 1.8 and 0.6 nm were deposited on 1.2 nm SiO_2/Si(100) at room temperature. The Si 2p, O 1s and Pr 3d core-level spectra were used to investigate the Pr/SiO_2/Si surfaces as a function of annealing temperature. The Pr overlayers reduce SiO_2, forming Pr_2O_3 and the Pr silicate. The silicate grows and the Pr_2O_3 intensity decreases with annealing temperature. For the 1.8 nm Pr/SiO_2/Si system, the SiO_2 layer can be reduced completely at room temperature and the Pr silicide as well as metallic Pr are present on the surface even after annealing. The Pr silicate becomes dominant after annealing at temperatures over 690 K. Angle-dependent XPS indicates that the silicate moves to the top surface. For the 0.6 nm Pr/SiO_2/Si system, some SiO_2 remains on the surface and almost all Pr atoms are bonded to oxygen after annealing.

References

[1] Schulz M 1999 *Nature* **399** 729
[2] Muller D A, Sorsch T, Moccio S, Baumann F H, Evans-Lutterodt K and Timp G 1999 *Nature* **399** 758
[3] Kingon A I, Maria J P and Streiffer S K 2000 *Nature* **406** 1032
[4] Wilk G D, Wallace R M and Anthony J M 2001 *J. Appl. Phys.* **89** 5243
[5] Wilk G D, Wallace R M and Anthony J M 2000 *J. Appl. Phys.* **87** 484
[6] Ono H and Katsumata T 2001 *Appl. Phys. Lett.* **78** 1832
[7] Liu J P, Zaumseil P, Bugiel E and Osten H J 2001 *Appl. Phys. Lett.* **79** 671
[8] Fissel A, Dąbrowski J and Osten H J 2002 *J. Appl. Phys.* **90** 8986
[9] Sayan S, Garfunkel E and Suzer S 2002 *Appl. Phys. Lett.* **80** 2135
[10] Liehr M, LeGoues F K, Rubloff G W and Ho P S 1985 *J. Vac. Sci. Technol.* A **3** 983
[11] Dadahai F, Gaspari F, Zukotynski S and Bland C 1996 *J. Appl. Phys.* **80** 6505
[12] Osten H J, Liu J P, Gaworzewski P, Bugiel E and Zaumseil P 2000 *Technical Digest Int. Electron Devices Mtg* (Piscataway, NJ: IEEE) p 653
[13] Briggs D and Seah M P 1983 *Practical Surface Analysis by Auger and X-ray Photoelectron Spectroscopy* (Chichester: Wiley)
[14] Tabe M, Chiang T T, Lindau I and Spicer W E 1986 *Phys. Rev.* B **34** 2706
[15] Iwata S and Ishizaka A 1996 *J. Appl. Phys.* **79** 6653
[16] Gunter P L J, de Jong A M, Niemantsverdriet J W and Rheiter H J H 1992 *Surf. Interface Anal.* **19** 161
[17] Saito Y, Yamaki K, Fujimori S, Suzuki S and Sato S 1999 *J. Electron Spectrosc. Relat. Phenom.* **101–103** 501